Modeling and Control of Hysteretic Deformable Mirror Bachelor Integration Project

M.A. Sluiter | S2999714 | m.a.sluiter@student.rug.nl | June 2021
First supervisor: Bayu Jayawardhana | Second supervisor: Mauricio Munoz Arias

I. Introduction

In terms of applying piezoelectric materials for actuating purposes, the ability to model the characteristic phenomena of the material is a fundamental milestone in precise control of the actuator. As unknown piezoelectric material may behave differently than the known counterparts, a first step in modeling the characteristic phenomena is obtaining extensive data on the behaviour by an experimental setup. Once the data is obtained, mathematical modeling is applied to get a first grasp at precise control of the actuating purposes. The research described in this report takes the same approach. As the research aims to build the Preisach model of a given piezoelectric actuator, where the model is to accurately describe the relation between the applied electric field and the corresponding strain, the research is divided into two parts. The first part focuses on obtaining the experimental data by running tests, the second part will be about applying mathematical modeling for building the Preisach model using the obtained data. This report provides the reader with documentation on both behalfs of the aforementioned approach. In the next paragraph the reader may find state of the art information on behalf of piezoelectric material and an application of its properties currently in development at the Rijksuniversiteit Groningen. As indicated, the first part of this report will contain the presentation of the experimental setup and the obtained results. After the presentation of the applied test setup and obtained measurements, the report will introduce the reader to key knowledge required for the mathematical modeling part of the research by describing the models which are aimed to be built. Next, the process of building the model is enlightened upon combined with an initial validation of the model. The report will conclude by an discussion on the experiments and the model supplemented with information on what future research may have to offer.

II. State of the Art

Adaptive optics is a scientific and engineering discipline whereby the performance of an optical system is improved by using information about the environment through which it passes [1]. One of the challenges the use of adaptive optics is applied in is extracting the optical information from beams of light traveling through the galaxies [2]. Incoming wavefront is distorted as a result of several factors, for example atmospheric turbulence and thermal blooming, referred to as aberrations. In order to achieve a clear and usable image, an adaptive optics system is applied. Adaptive optics have been used for imaging purposes through the atmosphere since 1982 [3]. Adaptive optics systems in general contain four basic components. By the use of a wavefront sampler, a wavefront sensor, a corrector which for example could be a deformable mirror and a control computer executing numerical calculations, distorted wavefront images are corrected into sharp images. The focus in this report lies on the component of adaptive optics systems which serves the purpose of correcting the wavefront, namely the deformable mirror. For a simplified schematic of adaptive optics systems, see figure 1.

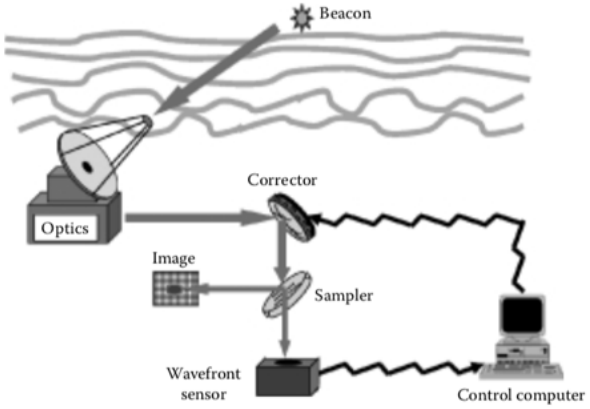

Fig. 1. General adaptive optics system schematically depicting all necessary elements for an operational system.

The deformable mirror element of the adaptive optics system is used to correct the wavefront. Deformable mirrors are generally described as continuous-surface mirrors with mechanically driven deformation by the use of actuators [4]. Generally speaking, deformable mirrors consist of a reflective surface membrane which undergoes deformation as a result of discrete actuators

perpendicular to the surface [1]. Commonly, piezoelectric ceramics are used as material for the deformable mirror discrete actuators. Basically, the piezoelectric ceramics provide the system with an actuator that is able to provide enough force to deform the mirror with accurate precision by converting an electrical signal into a precisely controlled displacement [5].

Deformable mirrors consist of a reflective surface acting as the mirror and multiple piezo actuators behind the reflective surface. For the use of deformable mirrors, the devices are designed with an as large as possible actuator number for optimal wavefront correction. This actuator number is often referred to as “pixels”. In the classic deformable mirror, each pixel is actuated by a piezo actuator having its own pair of cables. This for example applies in the state of the art deformable mirrors developed by Boston Micromachines Corporation and AOA Xinetics [6] [7].

To illustrate the problematics, in a 5x5 pixel classical deformable mirror, 25 piezo actuators are stationed behind the reflective surface and each of these actuators has its own pair of cables, resulting in 50 cables needed to operate this deformable mirror. Furthermore, as the piezoelectric material is used to achieve a desired deformation (strain), an electric field needs to be applied over this piezoelectric material. A limiting property of the classic deformable mirror is that to sustain the desired strain of the piezoelectric material, the electrical field over the piezoelectric material must remain constant at the desired level [8]. The combination of the many pairs of cables and the constant electric field required over each pixel in order to remain at desired strain results in problems and limitations. Microscale Inc. has specifically addressed the problem of extensive wiring. They have been developing deformable mirrors based on lead zirconate titanate in combination with ASIC boards in order to minimize the pixel wiring and reduce the mass of the system [9].

For the last couple of years, researchers from Netherlands Institute for Space Research (SRON), Zernike Institute for Advanced Materials (ZIAM) and Engineering and Technology Institute of Groningen (ENTEG) have been working on a high pixel number deformable mirror concept which utilizes piezoelectric hysteresis for stable shape configurations [10]. The development of the concept deformable mirror is highly interdisciplinary, each of the aforementioned institutes having its own area of expertise. ENTEG focuses on the development of the control, ZIAM focuses on piezo actuator development and SRON carries out overall management and takes care of engineering and nano technology. The team presents the conceptual design and initial development of the Hysteretic Deformable Mirror (HDM), see figure 2.

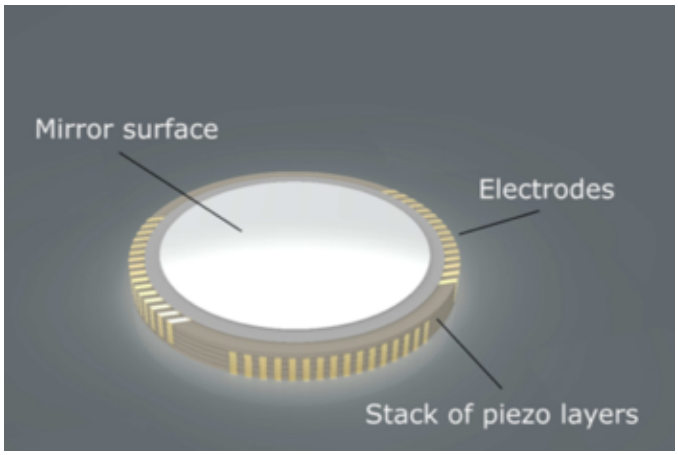

Fig. 2. HDM revolutionary conceptual design, indicating the combination of a stack of piezo layers and electrodes to actuate the mirror surface.

The Hysteretic Deformable Mirror reduces problems and increases functionality compared to the classic deformable mirror described prior in this section by two main properties and characteristics. The application of a specially developed highly hysteretic piezoelectric material combined with a simple electrode layout separates the Hysteretic Deformable Mirror from the classic deformable mirrors.

The combination of the implementation of these two properties give the Hysteretic Deformable Mirror a set-and-forget nature due to the large remnant property of the developed material [11]. This set-and-forget nature allows the Hysteric Deformable Mirror the use of time division multiplexing in order to address single pixels one by one without the need of retaining a constant electric field for each pixel due to the large remnant deformation property of the material. The use of strip electrodes minimizes the cables to a single cable per electrode. To illustrate this advantage, the 50 cables required for the classic 5x5 deformable mirror mentioned prior would reduce to only 10 cables in case of the HDM design applied to a 5x5 pixel layout. The limited number of electronics and wiring, combined with robust mechanical design, guarantees a lightweight and compact HDM system designed to be very robust to failure and vibration loads [10].

Modelling the hysteretic characteristics of the piezo material comes with a certain degree of complexity. The phenomenon of hysteresis has widely been studied and different approaches to describe it mathematically exist [12]. The Preisach hysteresis operator, due to its suitability to describe hysteresis in all kinds of physical phenomena, has been set as the chosen operator for modelling the hysteresis of the developed piezo material [13].

Presenting the relation between the electric field and the strain of the piezo actuators, including the remnant characteristics, the Preisach operator describes butterfly hysteresis loops used for surface shape modelling of the HDM [14].

With respect to the control strategy, the piezoelectric actuators are considered in a simplified model, where the actuators are modelled by a Preisach operator such as described above. In addition to this model a control loop is applied to drive each piezo actuator to the desired degree of deformation [15].

III. Experimental Setup

This paragraph will present the experimental setup used to obtain the experimental data for modeling the hysteretic behaviour of the piezoelectric material. Some remarks on behalf of the experimental procedure are stated in this paragraph as well. The used components of the setup are listed below. For clarifications on behalf of the attachments and interrelations of the components the reader is referred to the diagram depicted in figure 3.

The components of the setup are: PI P-611.2S Piezo stage for nanopositioning (Integrated SGS sensor), PI E-610 Piezo amplifier (voltage gain of 10), RS 724-430 Micrometer, Delta Electronics ES 030 power supply (constant supply of 15V), Delta Electronics E 018-0.6 D voltage controller (interval from 0V to 10V), Fluke 175 True Ams Multimeter, Fluke 8808A 5-1/2 Digit Multimeter.

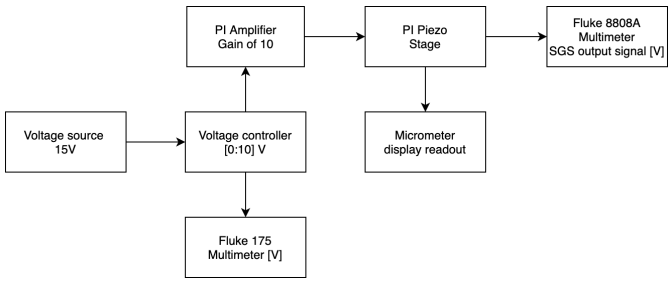

Fig. 3. Experimental setup used to obtain the measurement data. The used components described prior in this section are depicted including the connections.

If the voltage connected to the piezo stage is increased, strain will occur and linear deformation will be noticed and measured by the connected micrometer and integrated SGS sensor. The same goes for decreasing the voltage. If the voltage is decreased, the hysteretic behaviour of the piezo stage is noticed. Due to memory properties of the material the linear deformation goes back to its original state with a delay. Modeling this specific delay is the challenge of this experimental setup and the corresponding mathematical modeling.

The procedure is as follows: the initial voltage is 0V, with a corresponding linear deformation of zero. The voltage is increased by 5V each iteration, using the voltage controller and amplifier. After each increase of the voltage, the voltage output signal measured by the integrated SGS sensor and displayed by the Fluke 8808A multimeter as well as the linear deformation displayed by the micrometer is notated in a spreadsheet file. By steps of 5V the voltage is increased to 100V. Once 100V is reached, the voltage is reduced by the same amount of voltage with the same interval back to 0V, notating the output voltage signal and displayed deformation by the micrometer as well. The procedure is repeated 3 times to validate the measurements for irregularities. The results are presented and discussed in the next paragraph.

IV. Experimental results

This paragraph will present the reader the results of the experimental activities. The gathered data are depicted in the form of hysteresis loops. Two hysteresis loops obtained from the experimental activities are shown in figure 4 and 5.

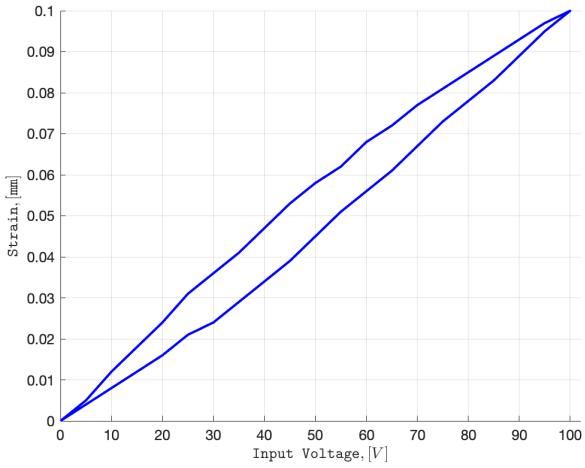

Fig. 4. The first obtained hysteresis loop, the output data being gathered by the use of a micrometer. Output in [mm].

Both loops display the same input voltage. In the first loop this input voltage is displayed against the [mm] readout of the micrometer, in the second loop the input voltage is displayed against the output voltage signal generated by the internal SGS. An additional element of the hysteresis loops is the presentation of time in the plot. As described in the prior paragraph, first the voltage would be increased from 0V to 100V after which it would decreased back to 0V. In both plots the lower

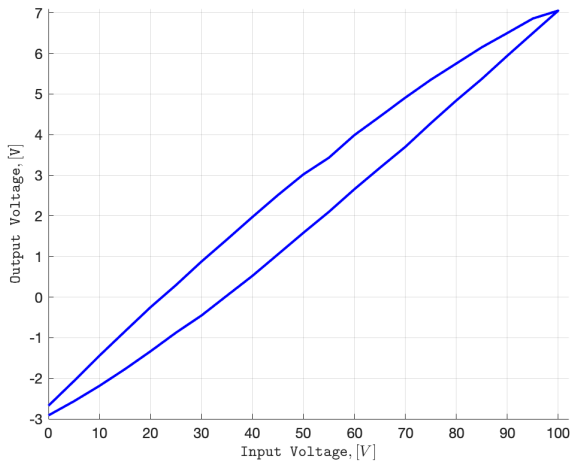

Fig. 5. The second obtained hysteresis loop, the output data being gathered by the use of the internal SGS. Output in [V].

line indicates the way up and the upper line indicates the way back.

Both plots show the same hysteretic behaviour, which one would expect since they display the same experimental activity but measured with different sensors. Furthermore, as stated in the prior paragraph, during the experiment the obtained measurements were notated in a spreadsheet file. The information in this spreadsheet is imported to MATLAB to generate the depicted plots. For the next phase of the research, as stated in the introductory paragraph and enlightened upon in the upcoming one, the obtained data should be integrated in MATLAB as well, since MATLAB will provide the digital environment for the mathematical modeling of the hysteresis.

V. Preisach Operator

As the reader has been introduced to prior in this report, the first part of the research aims at gathering experimental data from test activities, while the second part of the research aims at using the gathered experimental data by means of mathematical modelling to build the Preisach model. As the prior paragraphs display the results of the first part, this paragraph will provide the reader with preliminaries for the second part of the research, focussing on building the model.

As the complex behaviour of hysteresis will bring modeling it with a certain degree of difficulty, several models exist to describe the behaviour and eventually control the displacement. If one would divide these models into three kinds the models would be divided into the following three approaches: physical based, differential equation based and operator based models. For the purpose of this research, as mentioned in the state of the art paragraph, the initial model to be built would be the Preisach model, categorised as an operator based hysteresis model. The fundament for operator based hysteresis models was developed by Preisach himself (1935). The model makes use of a relay which is employed as an elementary operator. The relay operates by on and off switches depending on the values of α and β. In case of an off switch the output value would take the form of -1 and in case of an on switch the value would take the form of +1. The mathematical description of the relay operator is stated below.

$$\mathcal{R}_{\alpha,\beta}(u(t)) = \begin{cases} 1 & \text{if } u(t) \geq \alpha \\ -1 & \text{if } u(t) < \beta \\ \mathcal{R}_{\alpha,\beta}(u(t-T)) & \text{otherwise} \end{cases} \quad (1)$$

Besides relay operators, the Preisach model consists of the weight density function $\mu(\alpha,\beta)$ as well. This weight density function $\mu(\alpha,\beta)$ can be identified using the obtained experimental data and would be the first step in building the Preisach model. The mathematics of the hysteresis loop modeled by the Preisach operator are stated next.

$$\Phi(u) = \iint_{\alpha \geq \beta} \mu(\alpha,\beta)\mathcal{R}_{\alpha,\beta}(u)d\alpha d\beta \quad (2)$$

The initial goal of this research is to model the linear displacement x of the piezo stage by Preisach operator $\phi(u)$ with input signal $u(t)$. As stated in the paragraph concerning the experimental setup, the applied input signal $u(t)$ would be the voltage signal.

VI. Identification

The report is structured in such a way that first the experimental setup and the obtained results are presented after which the second part of the report focuses on building the Preisach model. This section elaborates on the first step of building the model, identification of the Preisach weight density function $\mu(\alpha,\beta)$.

As elaborated on in prior sections, the obtained measurement data is imported to MATLAB. This mathematical modeling environment is used for identification of the weight density function of the Preisach operator $\mu(\alpha,\beta)$. The procedure and mathematics are well described in literature [16] [17] [18]. Once the identification of the weight density function has been completed, the obtained hysteresis loop can be fitted using the model.

As with every numerical approach, a decision has to be made on the size of the grid that is created on the weighting function. This value is referred to as the discretization level M. As the value for M is increased, the fitting of the Preisach staircase curve becomes more accurate. In the procedure of the identification of $\mu(\alpha,\beta)$,

there is sought after the lowest value for M resulting in maximal accuracy in order to prevent over-fitting problems [19].

For the initial identification and fitting the chosen value for M equals 10. The results of the weight density function are depicted in figure 6, the corresponding fitting is depicted in figure 7. The error is calculated to be 8,45%.

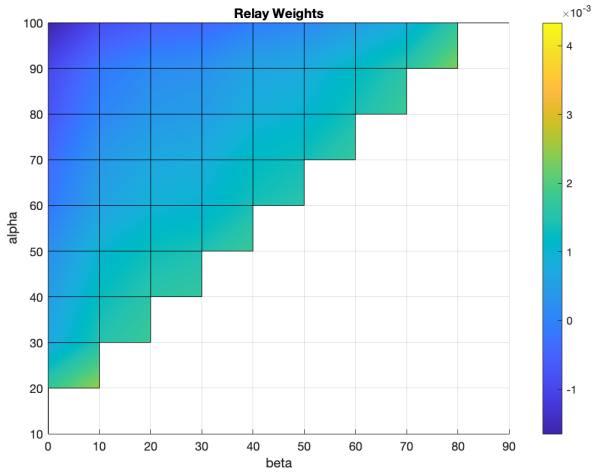

Fig. 6. Identification of the weight for discretization level M=10.

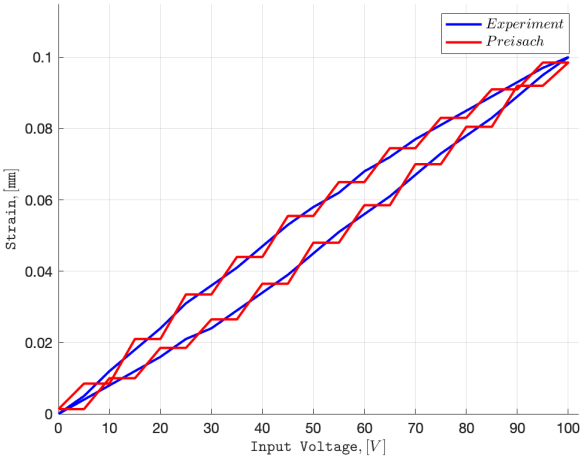

Fig. 7. Preisach operator fitting the experimental data for discretization level M=10. The error is calculated to be 8,45%.

As the value for M is increased the calculated error reduces. The lowest value for M indicating an error of 0% is determined to be 20. For M equals 20, the results of the weight density function are depicted in figure 8, the corresponding fitting is depicted in figure 9.

As the weight density function depicted in figure 8 is calculated to have a fitting error of 0% with the least amount of relays, this $\mu(\alpha,\beta)$ is used for the model.

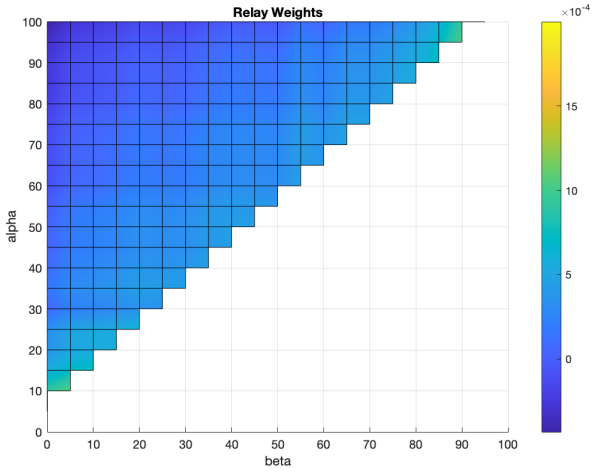

Fig. 8. Identification of the weight for discretization level M=20.

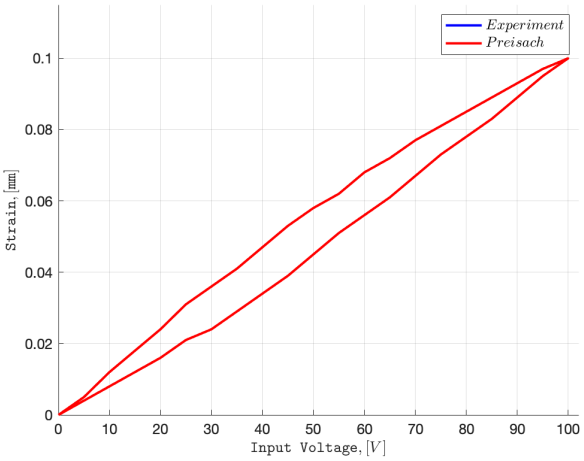

Fig. 9. Preisach operator fitting the experimental data for discretization level M=20. The error is calculated to be 0,00%.

VII. Validating the model

This section elaborates on the validation of the obtained model. The accuracy of the Preisach model can be validated by determining the degree of its ability to predict the hysteretic behaviour given a complex input sequence of voltage signals. Expected is that the model is not able to describe the complex input-output behaviour of the PI Piezo stage, since measurements funding the initial model come from straightforward voltage increments and decrements.

As there has been obtained an identification of the weight with a calculated error of 0,00%, the Preisach model is operationable. The $\mu(\alpha,\beta)$ depicted in figure 8 is applied. As the reader has been introduced to in the experimental setup and results sections, the hysteretic behaviour of the PI Piezo stage is measured by increasing the applied voltages 5V each iteration up to 100V and

back down to 0V. The measured deformation is plotted against the applied voltage resulting in the hysteresis loops depicted in figures 4 and 5 in the same sections. These measurement points are used to perform an identification of $\mu(\alpha,\beta)$ and therefore obtain a Preisach model aimed to accurately describe and predict the hysteretic behaviour of the aforementioned PI Piezo stage.

To validate the model, more complex measurements are gathered, making use of the same experimental setup described in section III. The procedure is similar as with the prior presented obtained measurement data, but the goal in this case is to obtain a hysteresis loop including several inner loops. The goal is to validate if the Preisach operator with $\mu(\alpha,\beta)$ as depicted in figure 8 is able to accurately predict these aforementioned inner loops.

The procedure for obtaining inner loops using the same experimental setup is as follows: the initial voltage is 0V, with a corresponding linear deformation of zero. The voltage is increased by 5V each iteration, notating the corresponding strain. Contrary to the first experiment, once a level of 30V is reached, the voltage is decreased by 5V each iteration back to 0V. This creates an inner loop. Once 0V has been reached, the voltage is increased again. The inner loop reduction in voltage is done twice once the voltage reaches 30V, 60V and 90V, each reducing the input voltage with an amount of 30V. The measurement results are depicted in figure 10.

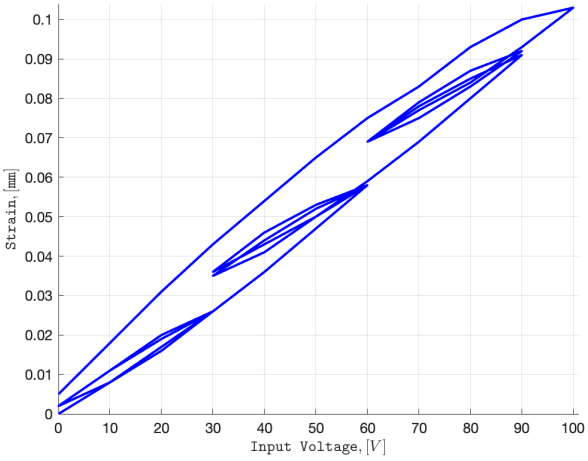

Fig. 10. Hysteresis loop obtained in same experimental setup depicting complex input-output behaviour in the form of two inner loops in the 0V-30V, 30V-60V and 60V-90V intervals.

If the model obtained in the identification section is given the same input sequence of voltage signals as depicted in figure 10, the Preisach operator will predict the hysteretic behaviour of the aforementioned PI Piezo stage. The Preisach operator predicts the displacement $\phi(u)$ with input sequence of voltage signals $u(t)$. The results of the model given the aforementioned input sequence of voltage signals are depicted in figure 11.

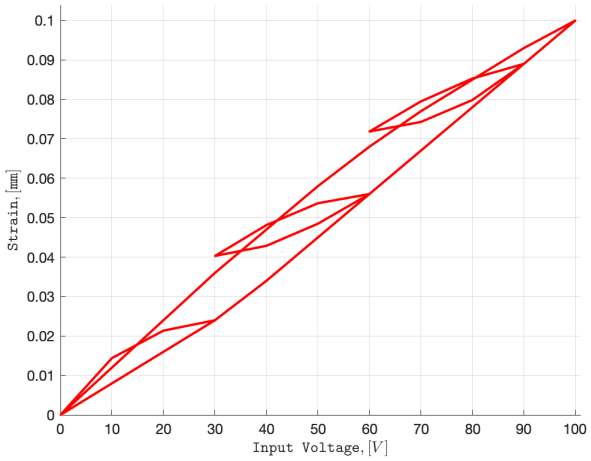

Fig. 11. Preisach operator $\boldsymbol{\phi(u)}$ against input sequence of voltage signals $\boldsymbol{u(t)}$. $\boldsymbol{\phi(u)}$ consisting of $\boldsymbol{\mu(\alpha,\beta)}$ as depicted in figure 8.

As the goal is to validate if the obtained Preisach operator is able to accurately predict a given complex input sequence of voltage signals, the results displayed in figure 10 and figure 11 are depicted together in figure 12. Plotted together one can conclude decent capability of $\phi(u)$ containing $\mu(\alpha,\beta)$ as depicted in figure 8 to predict complex input-output behaviour of the aforementioned PI Piezo stage. The error is calculated to be 11,83%.

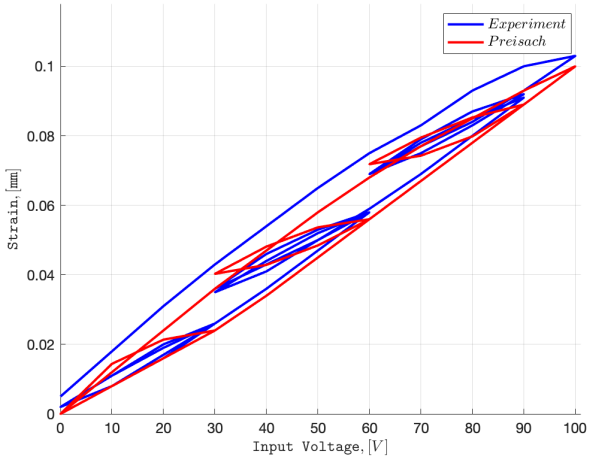

Fig. 12. Preisach operator $\boldsymbol{\phi(u)}$ and experimental results plotted against input sequence of voltage signals $\boldsymbol{u(t)}$.

VIII. Evaluation & Change

Analysing the obtained Preisach operator prediction given the aforementioned input sequence of voltage

signals depicted in figure 11, one can deduct from the plot that the inner loops in the 0V-30V, 30V-60V and 60V-90V intervals intersect with the major loop. In a functional Preisach operator the occurrence of these intersections is a reason to evaluate the applied approach for the identification of the weight density function $\mu(\alpha,\beta)$, since if the Preisach operator would behave as it is supposed to be, the intersections should not occur in the output prediction of the behaviour. Furthermore, as can be deduced from the plot in figure 10, the real life behaviour of the PI piezo stage given the same input sequence of voltage signals does not display any intersections either.

In the identification section two identifications of the weight density function $\mu(\alpha,\beta)$ are depicted in figure 6 and figure 8. As the fitting with the $\mu(\alpha,\beta)$ as depicted in figure 8 resulted in a calculated error of 0% in fitting the obtained measurements curve, $\mu(\alpha,\beta)$ as depicted in figure 8 is used for the Preisach operator validation as described in the section validating the model.

The identification of $\mu(\alpha,\beta)$ is achieved by performing a singular value decomposition on the obtained measurement data as depicted in figure 4. Since this initial singular value decomposition approach did not contain constraints, the identification of $\mu(\alpha,\beta)$ contains negative values. For elaboration on the negative values obtained in the identification of $\mu(\alpha,\beta)$ the reader is referred to figure 8, especially to the index on the right of the figure.

The aforementioned intersections between the inner loops and the major loop as depicted in figure 11 are a result of the negative values in $\mu(\alpha,\beta)$ as depicted in figure 8. To improve the obtained Preisach operator, the approach for the identification of $\mu(\alpha,\beta)$ is altered by replacing the singular value decomposition approach with a constrained linear least-squares approach, resulting in an identification of $\mu(\alpha,\beta)$ without negative values.

Similar as described in the identification section, the weight density function $\mu(\alpha,\beta)$ can be identified using the constrained linear least-squares approach, resulting in non-negative values for the relay weights. The lowest value for M indicating an error of 0% was determined to be 20. For M equals 20, the results of the weight density function are depicted in figure 13.

If the model obtained by the constrained linear least-squares approach, containing $\mu(\alpha,\beta)$ as depicted in figure 13, is given the same input sequence of voltage signals as depicted in figure 10, the Preisach operator will predict the hysteretic behaviour of the aforementioned PI Piezo stage. The Preisach operator predicts the displacement $\phi(u)$ with input sequence of voltage signals $u(t)$. The results of the model given the aforementioned input sequence of voltage signals are depicted in figure 14.

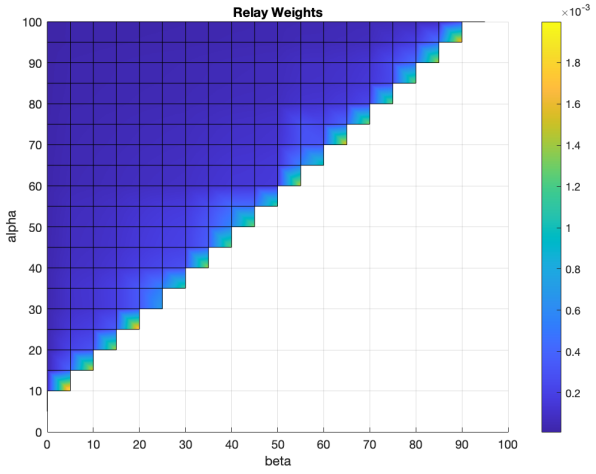

Fig. 13. Constrained identification of the weight for discretization level M=20.

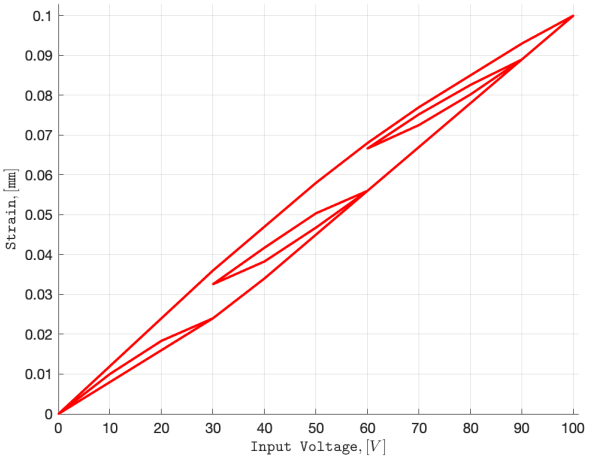

Fig. 14. Preisach operator $\boldsymbol{\phi(u)}$ against input sequence of voltage signals $\boldsymbol{u(t)}$. $\boldsymbol{\phi(u)}$ consisting of $\boldsymbol{\mu(\alpha,\beta)}$ as depicted in figure 13.

As the goal is to validate if the improved Preisach operator is able to accurately predict a given complex input sequence of voltage signals, the results displayed in figure 10 and figure 14 are depicted together in figure 15. Plotted together one can conclude similar capability of $\phi(u)$ containing $\mu(\alpha,\beta)$ as depicted in figure 13 to predict complex input-output behaviour of the aforementioned PI Piezo stage as with the case depicted in figure 12. Altering the approach for identification of $\mu(\alpha,\beta)$ by implementing constraints resulting in non-negative values for the relay weights eliminates the intersections as depicted in figure 11. The error is calculated to be 12,21%.

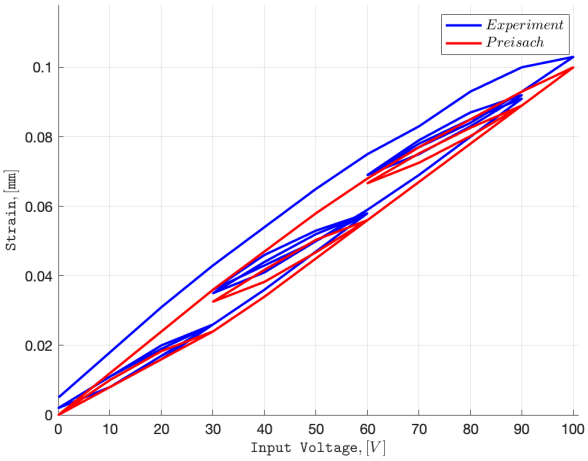

Fig. 15. Preisach operator $\phi(u)$ consisting of $\mu(\alpha,\beta)$ as depicted in figure 13 and experimental results plotted against input sequence of voltage signals $u(t)$.

IX. Discussion

As the overall goal presented in the report is to build a Preisach model to accurately predict the hysteretic behaviour of a given PI Piezo stage, two phases of this process can be deducted for evaluation. The first phase would be obtaining the behavioural measurements of the PI Piezo stage, the second phase would be creating the Preisach model by identification of the weight density function $\mu(\alpha,\beta)$ based on the obtained behavioural data. Both phases are up for discussion combined with elements of what future research may have to offer.

As in the current approach the experimental output had to be notated in a spreadsheet file, obtaining reliable data points is inefficient and time consuming. For a more accurate identification of the weight density function, each extra data point will make the model more accurate. Pursuing the goal of an accurate Preisach model, the experimental setup is aimed to be updated by automating the data acquisitions by implementing a National Instruments PCI6035E I/O board (DAQ). This update of the experimental setup will make gathering data easier and more efficient. If an initial model is obtained and the experimental setup has been improved by incorporating the DAQ, new data will be gathered in a much more extensive manner. By the use of this additional accurate information the initial model is aimed to be improved in such a way that it is able to accurately describe the complex input-output behaviour of the given PI piezo stage. Once the model is improved, it will be validated again. Furthermore, as described prior in the report, this research aims to model the linear displacement of the PI piezo stage against the input voltage signal. An additional improvement of the model would be to not model the linear displacement of the PI piezo stage against the input signal but to model the output force against the voltage input signal. Modeling the piezo in this way can be of contribution to the HDM development as described in the state of the art paragraph, since in this application the piezo actuators are stationed behind a mirror surface which is to be deformed by the piezo actuators.

References

[1] Tyson, R. K. (2015). Principles of adaptive optics. CRC press.
[2] Roddier, F. (Ed.). (1999). Adaptive optics in astronomy.
[3] Hardy, J. W. (1991, December). Adaptive optics: a progress review. In Active and Adaptive Optical Systems (Vol. 1542, pp. 2-17). International Society for Optics and Photonics
[4] Freeman, R. H., Pearson, J. E. (1982). Deformable mirrors for all seasons and reasons. Applied Optics, 21(4), 580-588
[5] Simonov, A. N., Hong, S., Vdovin, G. V. (2006). Piezoelectric deformable mirror with adaptive multiplexing control. Optical Engineering, 45(7), 070501
[6] Bifano, T. (2011). MEMS deformable mirrors. Nature photonics, 5(1), 21-23.
[7] Wirth, A., Cavaco, J., Bruno, T., Ezzo, K. M. (2013, May). Deformable mirror technologies at AOA Xinetics. In High-Power, High-Energy, and High-Intensity Laser Technology; and Research Using Extreme Light: Entering New Frontiers with Petawatt-Class Lasers (Vol. 8780, p. 87800M). International Society for Optics and Photonics
[8] Horenstein, M. N., Sumner, R., Miller, P., Bifano, T., Stewart, J., Cornelissen, S. (2011, February). Ultra-low-power multiplexed electronic driver for high resolution deformable mirror systems. In MOEMS and Miniaturized Systems X (Vol. 7930, p. 79300M). International Society for Optics and Photonics
[9] Prada, C. M., Yao, L., Wu, Y., Roberts Jr, L. C., Shelton, C., Wu, X. (2017, September). Characterization of low-mass deformable mirrors and ASIC drivers for high-contrast imaging. In Techniques and Instrumentation for Detection of Exoplanets VIII (Vol. 10400, p. 1040011). International Society for Optics and Photonics
[10] Huisman, R., Bruijn, M., Damerio, S., Eggens, M., Kazmi, S. N. R., Schmerbauch, A. E. M., ... Noheda, B. (2020). High pixel number deformable mirror concept utilizing piezoelectric hysteresis for stable shape configurations. arXiv preprint arXiv:2008.09338
[11] Damerio, S. (2017). Synthesis and implementation of piezoelectric materials as actuators for hysteretic deformable mirrors
[12] Hassani, V., Tjahjowidodo, T., Do, T. N. (2014). A survey on hysteresis modeling, identification and control. Mechanical systems and signal processing, 49(1-2), 209-233
[13] Gu, G. Y., Zhu, L. M., Su, C. Y., Ding, H., Fatikow, S. (2014). Modeling and control of piezo-actuated nanopositioning stages: A survey. IEEE Transactions on Automation Science and Engineering, 13(1), 313-332
[14] Schmerbauch, A. E. M., Vasquez-Beltran, M. A., Vakis, A. I., Huisman, R., Jayawardhana, B. (2020). Influence functions for a novel hysteretic deformable mirror with a high density 2D array of actuators. arXiv preprint arXiv:2005.07418
[15] Vasquez-Beltran, M. A., Jayawardhana, B., Peletier, R. (2020). Recursive algorithm for the control of output remnant of Preisach hysteresis operator. IEEE Control Systems Letters, 5(3), 1061-1066

[16] Stakvik, Jon Ragazzon, Michael Eielsen, Arnfinn Gravdahl, Jan. (2015). On Implementation of the Preisach Model Identification and Inversion for Hysteresis Compensation. Modeling, Identification and Control (MIC). 36. 133-142. 10.4173/mic.2015.3.1.

[17] Iyer, Ram Shirley, Matthew. (2004). Hysteresis Parameter Identification With Limited Experimental Data. Magnetics, IEEE Transactions on. 40. 3227 - 3239. 10.1109/TMAG.2004.833427.

[18] van de Beek, W. J. (2018). Operator-Based Modeling of Single Loop and Butterfly Hysteresis Phenomena in Piezoelectric Actuators

[19] Cawley, G. C., Talbot, N. L. (2010). On over-fitting in model selection and subsequent selection bias in performance evaluation. The Journal of Machine Learning Research, 11, 2079-2107.